



Gamma Irradiation of Cellulose Acetate-Polyethylene Glycol 400 Composite Membrane and Its Performance Test for Gas Separation

Arifina Febriasari¹, Meri Suhartini^{2*}, Ade L. Yunus², Rahmawati Rahmawati², Sudirman Sudirman³, Baity Hotimah⁴, Rika F. Hermana⁵, Sutrasno Kartohardjono¹, Aliya Fahira¹, Irma P. Permatasari¹

¹Department of Chemical Engineering, Faculty of Engineering Universitas Indonesia, Kampus UI Depok, Depok 16424, Indonesia

²Isotopes and Radiation Applications Technology Research Center, Research organization of Nuclear Power (BATAN)- National Nuclear Energy Agency – National Research and Innovation Agency, Jl. Lebak Bulus Raya No. 49, Jakarta 12440, Indonesia

³Nuclear Advance Material Research Center, National Nuclear Energy Agency – National Research and Innovation Agency, Puspitek, Serpong 15310, Indonesia

⁴Oil and Gas Technology Research and Development Center, Ministry of Energy and Mineral Resources, Cipulir 12230, Indonesia

⁵Department of Chemistry, Faculty of Mathematics and Natural Science, Pertamina University, Jakarta 12220, Indonesia

Abstract. Gas separation processes through membrane permeation have attracted the attention of researchers recently due to their promising applications. In this study, we modified the cellulose acetate (CA) membrane to improve the membrane performance of CO₂/CH₄ gas separation. The CA membrane was modified by adding polyethylene glycol (PEG) 400 as the carrier and *N, N'*-methylenebisacrylamide (MBA) as the cross-linking agent. Gamma-ray from cobalt 60 was used as a reaction initiator with variation in irradiation doses. The membrane characterization tests were conducted using scanning electron micrograph (SEM), Fourier transforms infrared (FTIR), and instron tensile strength tester. The permeability and selectivity of the membranes were tested against the single gases CO₂ and CH₄. The SEM analysis showed the morphology change in the membrane surface by gamma irradiation and a crosslinking agent. The spectra of FTIR showed a change in peak intensity on several polymer functional groups in the presence of gamma-ray irradiation. The tensile strength test showed that membranes with MBA have a higher mechanical strength than those without MBA. Based on the membrane permeability and selectivity tests, CO₂ gas permeability was affected by pressure. The ideal selectivity of CO₂/CH₄ shows that the irradiated membrane has a higher selectivity than that of the non-irradiated membrane.

Keywords: Cellulose acetate membrane; Fixed carrier membrane; Gamma irradiation; Gas separation; Polyethylene glycol

1. Introduction

Various types of technologies that can be applied for CO₂ gas separation have been investigated by many researchers, one of which is membrane technology (Kartohardjono et al, 2017; Kusrini et al, 2018; Yulia et al., 2019). Membrane separation technology was

*Corresponding author's email: meri001@brin.go.id, Tel.: +62-21-7690709; Fax.: +62-21-7691824
doi: [10.14716/ijtech.v12i6.5250](https://doi.org/10.14716/ijtech.v12i6.5250)

reported to have advantages, such as being environmentally friendly, having relatively low operating costs and low mobility, only requiring a compact space, and ease of maintenance and operation (Bandehali et al., 2020). The cellulose acetate (CA) membrane is one of the most widely used polymeric membranes for gas separation, including CO₂ and CH₄ gases. Pak et al. (2016) have investigated the use of the hollow fiber CA membrane to separate CO₂ and CH₄.

However, unmodified CA membranes tend to have a lower permeability to CO₂. Some researchers have reported that modified CA membranes could enhance CO₂ permeability (Sanaeepur et al., 2019). One of the compounds that can help increase the permeability of the CA membrane to CO₂ is polyethylene glycol (PEG) (Wu et al., 2015). CO₂ has a good solubility in PEG, so the addition of PEG can increase CO₂ permeability (Hu et al., 2006).

In this study, the modification of CA with PEG was carried out by adding *N,N'*-methylenebisacrylamide (MBA) as a cross-linking agent and performing gamma-ray irradiation (Suhartini et al., 2020). The aim of using the crosslinking agent was to improve the mechanical stability of the membrane at the time of application (Zhang et al., 2017; Pryhazhayeva et al., 2021).

The aim of this study was to examine the characteristics of the irradiated polymer membrane used for CO₂ gas separation. Gamma-ray irradiation increases the bond between CA, MBA, and PEG to form a copolymer that functions as a fixed carrier membrane (FCM) with the PEG molecule as the carrier. Ghobashy (2018) reported that the advantages of copolymerization irradiation are simple and safe methods. This method can accelerate the formation of polymer radicals so that it is easier for the copolymerization reaction to occur and to form a copolymer chain (Rahmawati et al., 2015). The aim of this study is to improve the performance of CA membranes with modifications using PEG as a carrier, MBA as a cross-linking agent, and gamma-ray irradiation as an accelerator for the bonding between CA, MBA, and PEG. Membrane casting was performed using the phase inversion method (Febriasari et al., 2021). The formed membrane was then characterized based on the Fourier transform infrared (FTIR) analysis, scanning electron micrograph (SEM), and tensile strength. The permeability and selectivity tests were conducted using single gases CO₂ and CH₄ to observe the membrane's performance.

2. Methods

2.1. Materials

The materials used in the experiment include cellulose acetate (M_n 30000) purchased from Sigma Aldrich Singapore. *N,N'*-methylenebisacrylamide, polyethylene glycol (M_w 400), acetone 99%, and formamide were purchased from Merck Indonesia.

2.2. Membrane Preparation

Cellulose acetate (CA) was dissolved into acetone and formamide with CA, acetone, and formamide mass ratios 1:2:1, respectively. The solution was stirred for 1 h until the CA was completely dissolved. Then, polyethylene glycol (PEG) was added in a ratio of 1:10 from the mass of CA. *N,N'*-methylenebisacrylamide (MBA) as a cross-linker agent was added with variations of 0 and 1% by weight of CA. The solution was again stirred until the PEG and MBA were completely dissolved for 1 h. The mixed solution was allowed to stand for one night to remove the bubbles then given gamma-ray irradiation using Cobalt-60 in a non-vacuum condition with a dose variation of 0 kGy, 5 kGy, 10 kGy, 15 kGy, and 25 kGy.

Membrane casting was executed by pouring the solution onto a glass plate and then printing it using a dr. Knife (casting membrane tool), and the thickness was set to 200 μm . The dope solution on the glass plate was allowed to stand at room temperature for 1 h and

was then put in a coagulation bath filled with demineralized water until a flat sheet membrane was formed. The flat sheet membrane was annealed using water with a temperature of 70°C for 10 min. The resulting membrane was then stored in a box containing demineralized water.

2.3. Membrane Characterization

Membrane characterization was conducted using a copolymerization degree analysis, functional group analysis, morphology test, crystallinity, thermal study, and mechanical properties. The copolymerization degree was measured to determine the percentage of PEG that binds to CA. The analysis was performed by comparing the membrane weight before and after the reflux process. The membrane sample was cut into a diameter of 1 cm and then wrapped in a stainless filter. The membranes were dried at 50°C for 1 h. Reflux was carried out using water for 48 h.

The FTIR analysis (Shimadzu, IR Prestidge-21) was performed to identify functional group changes as irradiation doses were increasingly administered to the membrane composite. FTIR spectra were observed at wave number 400-4000 cm⁻¹. The morphological analysis was performed to observe changes in the membrane surface structure due to the influence of irradiation doses and cross-linking agents. The membrane surface morphology test was performed using a scanning electron micrograph (SEM, JSM-6510LA, JEOL) with a magnification of 2000 times and a voltage of 30kV.

A tensile strength test was carried out to observe the mechanical properties of the membrane. The tensile test was conducted using the Universal Pull Machine. The value of the tensile strength was obtained using the following formula (Liu et al., 2013):

$$\sigma = \frac{F}{A_0} \quad (1)$$

where σ , F , and A_0 are tensile strength, loads during measurement, and surface area, respectively.

2.4. Permeability and Selectivity

The permeability and selectivity values of the membrane were measured using a set of membrane permeation test equipment with a membrane diameter of 5.1 cm. Single gas CO₂ and CH₄ flow with operational pressure variations from 0 to 50 Psi through the membrane permeation cell and the volume of the gas from the permeate were measured using a flow meter containing isopropanol. In this case, the distance and flow time of isopropanol were recorded for each pressure variation. Membrane permeability was observed by calculating the permeance using the following formula (Deng and Hägg 2010):

$$P/l = \left(\frac{Q_i}{A \times \Delta p_i} \right) \times 10^{-6} \quad (2)$$

P/l is permeance with GPU units, where 1 GPU = 1×10⁻⁶ cm³ (STP)/(cm² s cmHg). Q_i is the permeate flow rate for gas i in cm³(STP)/s. A is the effective surface area of the membrane (cm²), and Δp_i is the operational pressure (cmHg). The selectivity value (α) of the membrane was calculated using a comparison between the gas permeance values of CO₂ and CH₄ as in the following formula (Li et al., 2004):

$$\alpha = \frac{P_{CO_2}/l}{P_{CH_4}/l} \quad (3)$$

The scheme of the membrane performance test method is shown in Figure 1.

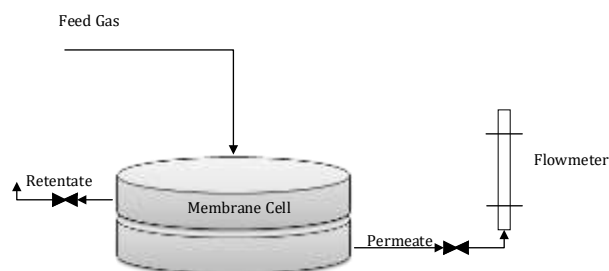


Figure 1 Scheme of the permeability test method

3. Results and Discussion

3.1. FTIR Spectra

Changes in membrane FTIR spectra due to an increase in irradiation doses and the effect of the cross-linking agent can be observed in Figure 2. The FTIR spectra show several peaks that identify polymer functional groups.

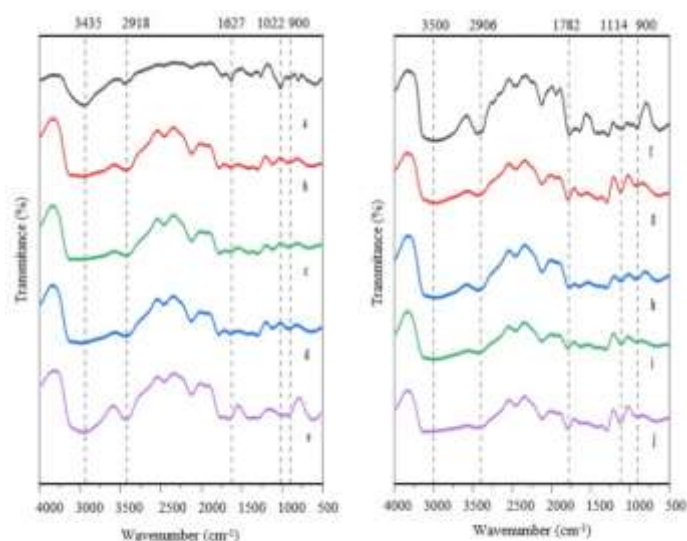


Figure 2 FTIR spectra of membranes. (a), (b), (c), (d), (e); CA-PEG with 0, 5, 10, 15, and 25 kGy irradiation doses, respectively. (f), (g), (h), (i), and (j); CA-MBA-PEG with 0, 5, 10, 15, and 25 kGy, respectively

Peaks that appear at the same wavenumber on each membrane indicate the existence of functional groups in the membrane sample. There was a change in the intensity and shape of the peak at some wave numbers. The CA-PEG membrane spectra were observed to change according to a variation in the irradiation dose. The reduced intensity at the 1627 cm⁻¹ peak indicates the degradation of the C=O carbonyl bond in the carboxyl group. Due to the opening of the C=O double bond, it is predicted to become a single radical bond, allowing CA to bind with PEG. The peak at wave number 3435 cm⁻¹ also experienced an intensity decrease in the irradiation dose from 5 to 15 kGy but increased again and was wider on the CA-PEG membrane with an irradiation dose of 25 kGy. The widening of the -OH bond peak indicates that more PEG binds to CA on the membrane with a dose of 25 kGy. The CA-MBA-PEG membrane spectra showed some peak shifts due to the CA-MBA interaction. The peak that appears at the wave number 3500 cm⁻¹ indicates an interaction of -OH groups with -NH from MBA (Waheed et al., 2014). The peak in the wavenumber of 1782 cm⁻¹ on the CA-MBA-PEG membrane with an irradiation dose of 5 and 25 kGy was noticeably sharper, indicating the addition of C=O carbonyl groups from MBA.

3.2. Membrane Morphology

The membrane surface morphology is presented in Figure 3. The SEM image shows changes in the membrane surface morphology due to the influence of irradiation and the effect of cross-linking agents on the membrane.

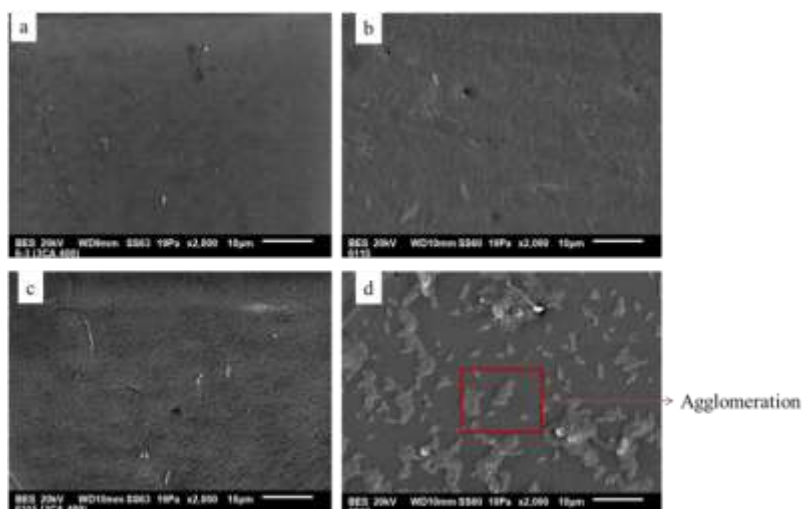


Figure 3 SEM image: (a) CA-PEG with 0 kGy irradiation dose; (b) CA-PEG with 10 kGy irradiation dose; (c) CA-PEG with 15 kGy irradiation dose; and (d) CA-MBA-PEG with 10 kGy irradiation dose

Figures 3a, 3b, and 3c show the effect of irradiation doses on the CA-PEG membrane without MBA. In contrast, Figure 2d shows the effect of the cross-linking agent on the irradiation treated membrane. CA and PEG 400 bind to each other at low doses of irradiation, resulting in molecular density. It causes a slight widening of the pores during the non-solvent induced phase inversion process, which was observed in the SEM results of irradiated CA-PEG membranes (Figures 3b and 3c) (Bedar et al., 2019).

The mixture of CA-PEG with the crosslinking agent MBA in the irradiated CA-MBA-PEG-10 kGy membrane allows the remaining PEG not to bind to CA so that agglomeration occurs on the membrane surface (Bedar et al., 2020). In this case, the CA and MBA molecules have pre-formed stable crosslinks. This makes it difficult for some PEG molecules to bond with CA and MBA so that agglomerations form on the membrane surface.

3.3. Tensile Strength

The results of the mechanical stability test obtained from the tensile strength analysis are presented in Figure 3.

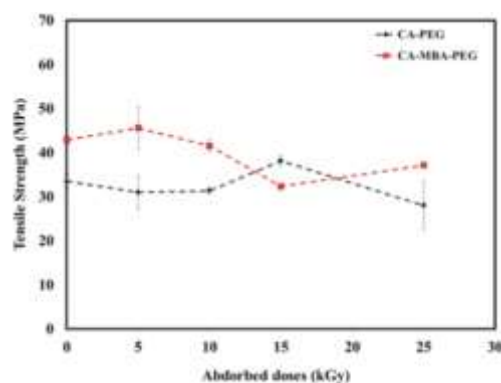


Figure 4 The membrane tensile strength as a function of the irradiation dose

One of the objectives of this experiment is to improve the mechanical stability of the membrane so that in addition to producing membranes with optimal affinities for CO₂ gas, this experiment also produced a membrane with a better mechanical strength. MBA is added in the membrane formation process as a crosslinking agent to increase the tensile strength (Kang et al., 2016). The experimental results shown in Figure 4 indicate the crosslinking agent's success in improving the membrane's mechanical properties.

Figure 3 also shows that the maximum tensile strength obtained on the CA-MBA-PEG membrane at a dose of 5 kGy. After decreasing the irradiation doses of 10 and 15 kGy, the tensile strength of the membrane then increased at a dose of 25 kGy. Meanwhile, the minimum tensile strength was observed in the CA-PEG membrane at a dose of 25 kGy. According to Shukla et al. (2016), the presence of a crosslinking agent reduces the crystallinity of a polymer membrane so that the tensile strength value is higher (Shukla et al., 2016).

The decrease in tensile strength on the membrane indicates that the crystallinity of the membrane is increasing. It may occur because the bond between CA and PEG in gamma-ray irradiation causes molecular density. This is in line with the results shown by the SEM analysis. The lower tensile strength of CA-MBA-PEG than CA-PEG for a 15 kGy irradiation dose was predicted to be due to the unstable bond between CA and MBA. At a certain dose of irradiation, there is a possibility of the homopolymerization of MBA, thus inhibiting its binding to CA.

3.4. Permeability and Selectivity

The results of the measurements and calculations of membrane permeability and ideal selectivity of CO₂ and CH₄ are shown in Figure 5. The gas permeation unit (GPU) describes how much CO₂ gas can penetrate the membrane and release into the permeate phase. In other words, it indicates the permeability of CO₂ gas to the membrane (Tocci et al., 2014; Wang et al., 2018). CO₂ gas permeability is affected by the solubility of CO₂ to the membrane. In this case, the copolymerization of CA with PEG is expected to increase the solubility of CO₂ to the membrane so that the membrane permeability increases (Reijerkerk et al., 2011). Gamma-ray irradiation and the presence of a crosslinking agent in this case help stabilize the bond between PEG and CA so that at certain irradiations, a more stable CA-MBA-PEG bond is formed.

The experimental results showed that the permeability of CO₂ is higher (0.36 to 13 GPU) than that of CH₄ (0.06 to 3.5 GPU). This proves the prediction that the presence of PEG in the blend membrane increases the permeability of CO₂ gas due to the higher solubility of CO₂ gas to PEG (Car et al., 2008). In the irradiated CA-PEG membrane, CO₂ permeance is higher (0.59 to 5.6 GPU) than that of the non-irradiated CA-PEG membrane (0.36 to 1.65 GPU). This indicates that the application of gamma-ray irradiation to the CA-PEG membrane causes more PEG molecules to bind to CA molecules. The stable bond between CA and PEG causes PEG not to be easily separated during the casting process or storage of the membrane. Compared with other studies that use membranes for CO₂ gas separation, Mubashir et al. (2019) used a mixed matrix membrane with NH₂-MIL-53(Al)/CA material and obtained CO₂ permeance values with a range of 1.22 to 2.74 GPU and a CO₂/CH₄ selectivity range of 19 to 39. Jahan et al. (2018) used membranes with cellulose/PVA nanocomposite materials and obtained CO₂ permeance values with a range of 0.04 to 0.28 GPU and a CO₂/CH₄ selectivity range of 4.2 to 14.4.

A significant increase in CO₂ gas permeability at pressures above 20 Psi was experienced by irradiated CA-PEG, non-irradiated CA-MBA-PEG membranes, and irradiated CA-MBA-PEG membranes. This is related to the phenomenon of CO₂-induced plasticization, which usually occurs in membranes made from glassy polymers (Zhang et al., 2010). This

experiment indicated that the addition of MBA and gamma-ray irradiation could reduce this effect.

Based on the calculation of membrane selectivity, the results show that at the pressure above 10 Psi, the CA-MBA-PEG and CA-PEG membranes given gamma-ray irradiation have a higher selectivity to non-irradiated membranes. Although non-irradiated CA-MBA-PEG has a higher CO₂ permeability, its selectivity is lower (3.75 to 24) than an irradiated CA-MBA-PEG membrane (8.5 to 114). This is due to the non-irradiated CA-MBA-PEG membrane, which is also has a high value for CH₄ gas permeability, so selectivity is low. In addition, the membrane with the addition of the MBA crosslinking agent has a higher selectivity compared to the CA-PEG membrane without MBA. These results prove that gamma-ray irradiation and the presence of crosslinking agents lead to a more stable PEG bond to the membrane, improving the membrane's performance.

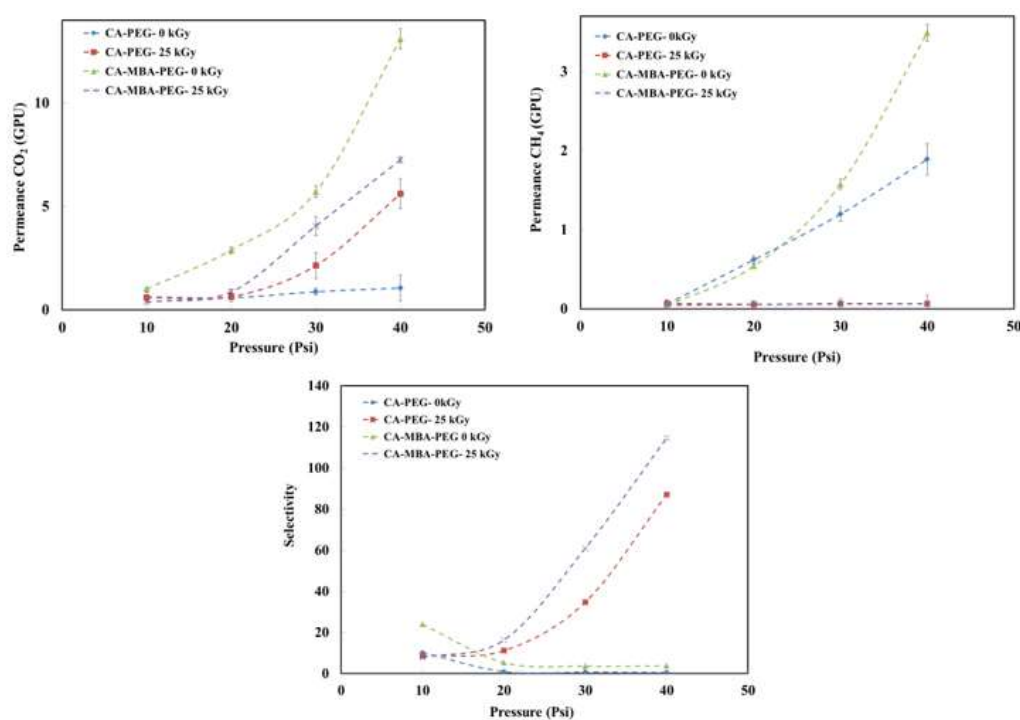


Figure 5 Membrane permeability and selectivity profiles against single gases CO₂ and CH₄

4. Conclusions

The copolymerization of CA-PEG and CA-MBA-PEG has been carried out using gamma-ray irradiation to form FCM. The Fourier transforms infrared (FTIR) results indicate that the irradiation process opened the carbonyl bonds in the CA molecule and changed the intensity of some peaks. The SEM analysis showed that gamma ray irradiation has the potential to widen the membrane pores due to the increase in molecular density caused by the intermolecular bonding process. The mechanical test results with tensile strength show that the CA-MBA-PEG membrane has a higher tensile strength value than that of the CA-PEG membrane. The membrane performance test on single gas CO₂ and CH₄ showed that the ideal selectivity of the CA-PEG and CA-MBA-PEG irradiated membranes was higher than that of the non-irradiated membranes. Ultimately, it can be concluded that this experiment produces a membrane that is quite selective for CO₂ with good stability against pressure. For further research, it is necessary to test the efficiency of the membrane against mixed gases and the stability of the membrane against changes in temperature.

Acknowledgements

The authors would like to thank the International Atomic Energy Agency (IAEA) for funding this research. Also, thanks to Mr. Mujiono and Mr. Tavip Sugeng Sugiono from Radiation and Isotopes Application Technology Research Center - Research Organization of Nuclear Power (BATAN)-BRIN for their practical help in this work

References

- Bandehali, S., Moghadassi, A., Parvizian, F., Hosseini, S.M., Matsuura, T., Joudaki, E., 2020. Advances in High Carbon Dioxide Separation Performance of Poly (Ethylene Oxide)-Based Membranes. *Journal of Energy Chemistry*, Volume 46, pp. 30–52
- Bedar, A., Goswami, N., Singha, A.K., Kumar, V., Debnath, A.K., Sen, D., Aswal, V.K., Kumar, S., Dutta, D., Keshavkumar, B., 2020. Nanodiamonds as a State-of-the-Art Material for Enhancing the Gamma Radiation Resistance Properties of Polymeric Membranes. *Nanoscale Advances*, Volume 2(3), pp. 1214–1227
- Bedar, A., Lenka, R., Goswami, N., Kumar, V., Debnath, A., Sen, D., Kumar, S., Ghodke, S., Tewari, P., Bindal, R., Kar, S., 2019. Polysulfone–ceria Mixed-Matrix Membrane with Enhanced Radiation Resistance Behavior. *ACS Applied Polymer Materials*, Volume 1(7), pp. 1854–186
- Car, A., Stropnik, C., Yave, W., Peinemann, K.V., 2008. PEG Modified Poly (Amide-B-Ethylene Oxide) Membranes for CO₂ Separation. *Journal of Membrane Science*, Volume 307(1), pp. 88–95
- Deng, L., Hägg, M.B., 2010. Swelling Behavior and Gas Permeation Performance of PVAm/PVA Blend FSC Membrane. *Journal of Membrane Science*, Volume 363(1-2), pp. 295–301
- Febriasari, A., Huriya, Ananto, A.H., Suhartini, M., Kartohardjono, S., 2021. Polysulfone–Polyvinyl Pyrrolidone Blend Polymer Composite Membranes for Batik Industrial Wastewater Treatment. *Membranes*, Volume 11(1), pp. 1–17
- Hu, X., Tang, J., Blasig, A., Shen, Y., Radosz, M., 2006. CO₂ Permeability, Diffusivity and Solubility in Polyethylene Glycol-Grafted Polyionic Membranes and Their CO₂ Selectivity Relative to Methane and Nitrogen. *Journal of Membrane Science*, Volume 281(1-2), pp. 130–138
- Jahan, Z., Niazi, M.B.K., Hägg, M.-B., Gregersen, Ø.W., 2018. Cellulose Nanocrystal/PVA Nanocomposite Membranes for CO₂/CH₄ Separation at High Pressure. *Journal of Membrane Science*, Volume 554, pp. 275–281
- Kang, N., Shin, J., Hwang, T.S., Lee, Y.S., 2016. A Facile Method for the Preparation of Poly(Vinylidene Fluoride) Membranes Filled with Cross-Linked Sulfonated Polystyrene. *Reactive and Functional Polymers*, Volume 99, pp. 42–48
- Kusrini, E., Utami, C.S., Usman, A., Nasruddin, Tito, K.A., 2018. CO₂ Capture using Graphite Waste Composites and Ceria. *International Journal of Technology*, Volume 9(2), pp. 291–319
- Kartohardjono, S., Paramitha, A., Putri, A.A., Andriant, R., 2017. Effects of Absorbent Flow Rate on CO₂ Absorption through a Super Hydrophobic Hollow Fiber Membrane Contactor. *International Journal of Technology*, Volume 8(8), pp. 291–319
- Li, Y., Cao, C., Chung, T.-S., Pramoda, K.P., 2004. Fabrication of Dual-Layer Polyethersulfone (PES) Hollow Fiber Membranes with an Ultrathin Dense-Selective Layer for Gas Separation. *Journal of Membrane Science*, Volume 245(1), pp. 53–60
- Liu, J., Lu, X., Wu, C., 2013. Effect of Preparation Methods on Crystallization Behavior and Tensile Strength of Poly (Vinylidene Fluoride) Membranes. *Membranes*, Volume 3(4), pp. 389–405

- Mubashir, M., Yeong, Fong, Y., Chew, Leng, T., Lau, Keong, K., 2019. Optimization of Spinning Parameters on the Fabrication of NH₂-MIL-53(Al)/Cellulose Acetate (CA) Hollow Fiber Mixed Matrix Membrane for CO₂ Separation. *Separation and Purification Technology*, Volume 215, pp. 32–43
- Pak, S-H., Jeon, Y-W., Shin, M-S., Koh, H.C., 2016. Preparation of Cellulose Acetate Hollow-Fiber Membranes for CO₂/CH₄ Separation. *Environmental Engineering Science*, Volume 33(1), pp. 17–24
- Pryhazhayeva, L., Shunkevich, A., Polikarpov, A., Krul, L., 2021. Synthesis and Long-Term Stability of Acrylic Acid and N, N-Methylene-Bis-Acrylamide Radiation Grafted Polypropylene Fibers. *Journal of Applied Polymer Science*, Volume 138(32), <https://doi.org/10.1002/app.50805>
- Rahmawati., Suhartini, M., Budiarto, E., 2015. Radiation Graft Copolymerization of Acrylic Acid onto Rice Straw Cellulose. *Macromolecular Symposia*, Volume 353(1), pp. 231–239
- Reijerkerk, S.R., Nijmeijer, K., Ribeiro Jr, C.P., Freeman, B.D., Wessling, M., 2011. On the Effects of Plasticization in CO₂/Light Gas Separation using Polymeric Solubility Selective Membranes. *Journal of Membrane Science*, Volume 367(1-2), pp. 33–44
- Sanaeepur, H., Ahmadi, R., Sinaei, M., Kargari, A., 2019. Pebax-Modified Cellulose Acetate Membrane for CO₂/N₂ Separation. *Journal of Membrane Science and Research*, Volume 5(1), pp. 25–32
- Shukla, P., Bajpai, A., Bajpai, R., 2016. Structural, Morphological, Thermal and Mechanical Characterization of Cellulose Acetate–Poly (Acrylonitrile) Semi Interpenetrating Polymer Network (IPN) Membranes and Study of Their Swelling Behavior. *Polymer Bulletin*, Volume 73(8), pp. 2245–2264
- Suhartini, M., Ernawati, E.E., Roshanova, A., Haryono, H., Mellawati, J., 2020. Cellulose Acetate of Rice Husk Blend Membranes: Preparation, Morphology and Application. *Indonesian Journal of Chemistry*, Volume 20(5), pp. 1061–1069
- Tocci, E., De Lorenzo, L., Bernardo, P., Clarizia, G., Bazzarelli, F., Mckeown, N.B., Carta, M., Malpass-Evans, R., Friess, K., Pilnáček, K.T., 2014. Molecular Modeling and Gas Permeation Properties of a Polymer of Intrinsic Microporosity Composed of Ethanoanthracene and Tröger's Base Units. *Macromolecules*, Volume 47(22), pp. 7900–7916
- Waheed, S., Ahmad, A., Khan, S.M., Jamil, T., Islam, A., Hussain, T., 2014. Synthesis, Characterization, Permeation and Antibacterial Properties of Cellulose Acetate/Polyethylene Glycol Membranes Modified with Chitosan. *Desalination*, Volume 351, pp. 59–69
- Wang, S., Tian, Z., Dai, S., Jiang, D.-E., 2018. Effect of Pore Density on Gas Permeation through Nanoporous Graphene Membranes. *Nanoscale*, 10(30), pp. 14660–14666
- Wu, X.M., Zhang, Q.G., Lin, P.J., Qu, Y., Zhu, A.M., Liu, Q.L., 2015. Towards Enhanced CO₂ Selectivity of the PIM-1 Membrane by Blending with Polyethylene Glycol. *Journal of Membrane Science*, Volume 493, pp. 147–155
- Yulia, F., Utami, V.J., Nasruddin, Zulys, A., 2019. Synthesis, Characterizations, and Adsorption Isotherms of CO₂ on Chromium Terephthalate (MIL-101) Metal-Organic Frameworks (Mofs). *International Journal of Technology*, Volume 10(7), pp. 1427–1436
- Zhang, H., Huang, X., Jiang, J., Shang, S., Song, Z., 2017. Hydrogels with High Mechanical Strength Cross-Linked by a Rosin-Based Crosslinking Agent. *RSC Advances*, Volume 7(67), pp. 42541–42548
- Zhang, L., Xiao, Y., Chung, T.-S., Jiang, J., 2010. Mechanistic Understanding of CO₂-Induced Plasticization of a Polyimide Membrane: A Combination of Experiment and Simulation Study. *Polymer*, Volume 51(19), pp. 4439–4447